



Recent results on charm physics at BESIII

Hai-Bo Li (for BESIII Collaboration)

Institute of High Energy Physics, Yuquan Road 19-2, Beijing 100049, China

Abstract

About 2.9 fb^{-1} data set had been collected with the BESIII detector at the BEPCII collider. Taking advantages of data near open-charm threshold, we present preliminary results on leptonic and semileptonic charm-meson decays, as well as result on the FCNC process $D^0 \rightarrow \gamma\gamma$ from BESIII experiment. High precision charm data will enable us to validate Lattice QCD calculations at the few percent level. These can then be used to make precise measurements of CKM elements, V_{cd} and V_{cs} , which are useful to improve the accuracy of test of the CKM unitary.

Keywords: Leptonic decay; Semileptonic decay; Rare charm decay

1. Introduction

The charm physics potential at open-charm threshold plays important role on quark flavor physics [1]. The open-charm program at BESIII includes studies of leptonic, semileptonic, hadronic charm-meson decays, searches for neutral D mixing, CP violations, and rare and forbidden charm decays, which are sensitive to physics beyond standard Model (SM). The quark mixing parameters are fundamental constants of the SM. They determine the nine weak-current quark coupling elements of the CKM matrix [2]. Studies of the semileptonic or pure-leptonic decays of D mesons are preferred way to determine the CKM elements, $|V_{cs}|$ and $|V_{cd}|$, since the strong interaction binding effects are parameterized by form factors or decay constants that are calculable, for example, by lattice QCD (LQCD) and QCD sum rules. On the other hand, $|V_{cs}|$ and $|V_{cd}|$ are tightly constrained when CKM matrix is assumed to be unitary. Therefore, measurements of charm semileptonic or pure-leptonic decay rates rigorously test theoretical prediction of the D meson semileptonic form factors or decay constants. High precision predictions of QCD will then remove road blocks for many weak and flavor physics measurements, such as in B decays for determinations of $|V_{ub}|$ and neutral B mixing parameters.

Many of the measurements related to charm decays

are also accessible to the B-factories and Super-B factories. What are the advantages to running at the open charm threshold at the BESIII experiment? The BESIII experiment will not be able to compete Super-B factories in statistics on charm physics, especially on the rare and forbidden decays of charm mesons. However, data taken at charm threshold still have powerful advantages over the data at $\Upsilon(4S)$, which we list here [1, 3]: 1) Charm events produced at threshold are extremely clean; 2) the measurements of absolute branching fraction can be made by using double tag events, which was first applied by the MARKIII Collaboration at SPEAR [4]. The produced $\psi(3770)$ in our sample decays into a pair of $D\bar{D}$. Reconstructing one of the D mesons with know exclusive hadronic modes while looking for decays of the other D mesons would allow us to reconstruct final states with neutrinos; 3) signal/Background is optimum at threshold; 5) Quantum coherence allow simple [5] and complex [6] methods to measure $D^0\bar{D}^0$ mixing parameters, direct CP violation and strong phase differences.

In this talk, I report preliminary results on charm meson decays based on a sample collected at the BEPCII with the BESIII detector [7]. This sample was collected at $\sqrt{s} = 3.773 \text{ GeV}$ with an integrated luminosity of 2.9 fb^{-1} in which the background levels at the open charm

threshold is expected to be substantially lower than that at the $\Upsilon(4S)$ peak at B factories.

2. Purely leptonic D decay

With a sample of 2.9 fb^{-1} taken at open-charm threshold, BESIII experiment measures the decay branching fraction for $D^+ \rightarrow \mu^+ \nu_\mu$ and extracts decay constant f_{D^+} [8]. Decay constant characterizes the strong-interaction physics at the quark-annihilation vertex. In a fully leptonic decay, they parameterize all of our essential theoretical limitations. Decay constant for B case also appears in the evaluation of box diagrams, and limit theoretical precision in calculating the neutral B meson mixing. Thus, lack of knowledge of the B^0 and B_s decays constants limits the usefulness of precise measurements of $B^0 - \bar{B}^0$ and $B_s - \bar{B}_s$ oscillations. These mixing data are our best sources of information on the CKM matrix elements V_{td} and V_{ts} , which are difficult to measure directly in top decay. The leptonic decay of charm meson presents an opportunity to check LQCD results for decay constants against precision measurements.

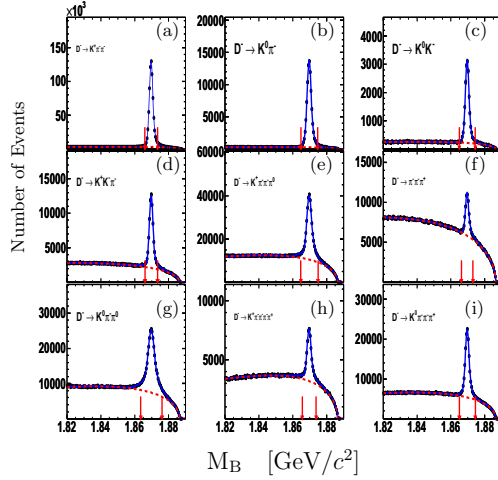


Figure 1: Distributions of the beam energy constraint masses for D^- hadronic tags used for the $D^+ \rightarrow \mu^+ \nu$ analysis. Modes in panels (a)-(i) are $D^- \rightarrow K^+ \pi^- \pi^-$, $K_S \pi^-$, $K_S K^-$, $K^+ K^- \pi^-$, $K^+ \pi^- \pi^- \pi^0$, $\pi^+ \pi^- \pi^-$, $K_S \pi^- \pi^0$, $K^+ \pi^- \pi^- \pi^- \pi^+$, and $K_S \pi^- \pi^- \pi^+$.

A tag is simply a fully-reconstructed D hadronic decays. A sample of tagged events has greatly reduced background and constrained kinematics, both of which aid studies of how the other D in the event decays. One can infer neutrinos from energy and momentum conservation, allowing full reconstruction of (semi)leptonic D decays. The typical tag rates per D (not per pair)

are roughly 15% and 10% for D^0 and D^+ , respectively. For pure leptonic decay in this analysis, the singly tagged D^- mesons are reconstructed in nine non-leptonic decay modes of $D^- \rightarrow K^+ \pi^- \pi^-$, $K_S \pi^-$, $K_S K^-$, $K^+ K^- \pi^-$, $K^+ \pi^- \pi^- \pi^0$, $\pi^+ \pi^- \pi^-$, $K_S \pi^- \pi^0$, $K^+ \pi^- \pi^- \pi^- \pi^+$, and $K_S \pi^- \pi^- \pi^+$. Mass peaks for the nine hadronic tag modes are shown in Fig. 1. A maximum likelihood fit to the mass spectrum yields the number of the singly tagged D^- events for each of the nine modes. The total number of tagged D^- events are $1565953 \pm 2327 D^-$.

The chosen signal variable for the $\mu^+ \nu$ decay is the calculated square of the missing-mass of any undetected decay products, shown in Fig. 2; this should of course peak at $M_\nu^2 = 0$ for signal events. The power of D -tagging is evident in the clean, isolated signal peak. In Table 1, sources of background modes are summarized including $K_L \pi^+$, $\pi^+ \pi^0$, $\tau \nu$ and other components. After

Table 1: Sources of background events for $D^+ \rightarrow \mu \nu$.

Source mode	Number of events
$D^+ \rightarrow K_L \pi^+$	7.9 ± 0.8
$D^+ \rightarrow \pi^+ \pi^0$	3.8 ± 0.5
$D^+ \rightarrow \tau^+ \nu$	6.9 ± 0.7
Other D decays	17.9 ± 0.1
ISR to ψ' and J/ψ	0.2 ± 0.2
$\psi(3770) \rightarrow \text{Non-}D\bar{D}$	0.9 ± 0.4
$e^+ e^- \rightarrow q\bar{q}$	8.2 ± 1.4
$e^+ e^- \rightarrow \tau^+ \tau^-$	1.9 ± 0.5
Total	47.7 ± 2.3

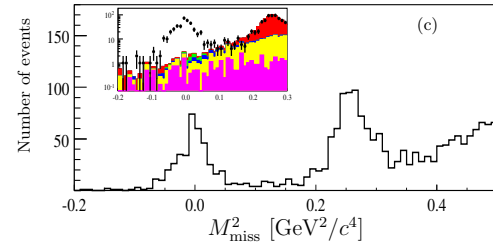


Figure 2: BESIII missing-mass-squared plot for $D^+ \rightarrow \mu^+ \nu$. The insert shows the signal region on a vertical log scale, where dots with error bars are for the data, histograms are for the simulated backgrounds from $D^+ \rightarrow K_L \pi^+$ (red), $D^+ \rightarrow \pi^+ \pi^0$ (green), $D^+ \rightarrow \tau^+ \nu$ (blue) and other decays of D mesons (yellow) as well as from $e^+ e^- \rightarrow \text{non-}D\bar{D}$ decays (pink).

subtracting the expected number of background events, about 377.3 ± 20.6 signal events for $D^+ \rightarrow \mu^+ \nu$ decay are retained, where the error is statistical. The overall efficiency for observing the decay $D^+ \rightarrow \mu^+ \nu$ is determined to be 63.82% by analyzing full Monte Carlo (MC) sim-

ulation events of $D^+ \rightarrow \mu^+ \nu$ versus D^- tags. Therefore, we obtain the preliminary branching fraction to be

$$\mathcal{B}(D^+ \rightarrow \mu^+ \nu) = (3.74 \pm 0.21 \pm 0.06) \times 10^{-4}, \quad (1)$$

where the first error is statistical and the second systematic. This measured branching fraction is consistent within error with world average of $\mathcal{B}(D^+ \rightarrow \mu^+ \nu) = (3.82 \pm 0.33) \times 10^{-4}$ [9], but with more precision. The decay constant f_{D^+} is then obtained using 1040 ± 7 fs as the D^+ lifetime and 0.2256 as V_{cd} [9]. Our preliminary result is

$$f_{D^+} = (203.91 \pm 5.72 \pm 1.97) \text{ MeV}, \quad (2)$$

where the first errors are statistical and the second systematic arising mainly from the uncertainties in the measured branching fraction (1.7%), the CKM matrix element V_{cd} (0.3%), and the lifetime of the D^+ meson (0.7%) [9]. The total systematic error is 1.0%. In Table 2, the BESIII preliminary results are compared with CLEO-c [10] and LQCD predictions [11] for the decay constant. The preliminary result from BESIII is the best number in the context of the SM, and remains consistent with LQCD.

Table 2: Comparison of results for $D^+ \rightarrow \mu \nu$ and decay constant from BESIII [8], CLEO-c [10] and LQCD prediction [11].

Model	$\mathcal{B}(D^+ \rightarrow \mu^+ \nu) \times 10^{-4}$	f_{D^+} (MeV)
BESIII	$3.74 \pm 0.21 \pm 0.06$	$203.91 \pm 5.72 \pm 1.97$
CLEO-c [10]	$3.82 \pm 0.32 \pm 0.09$	$205.8 \pm 8.5 \pm 2.5$
Average	3.76 ± 0.18	204.5 ± 5.0
HPQCD [11]	-	213 ± 4

3. Semileptonic D decays: $D^0 \rightarrow K^- e^+ \nu$ and $\pi^- e^+ \nu$

One of the best ways to measure magnitudes of CKM elements is to use semileptonic decays since they are far simpler to understand than hadronic decays and the decay width is $\sim |V_{cq}|^2$. On the other hand, measurements using other techniques have obtained useful values for V_{cs} and V_{cd} [12], and thus semileptonic D decay measurements are a good laboratory for testing theories of QCD. For a D meson decaying into a single hadron (h), the decay rate can be written exactly in terms of the four-momentum transfer defined as:

$$q^2 = (p_D^\mu - p_h^\mu)^2 = m_D^2 + m_h^2 - 2E_h m_D. \quad (3)$$

For decays to pseudoscalar mesons and virtually massless leptons, the decay width is given by:

$$\frac{d\Gamma(D \rightarrow P e^+ \nu)}{dq^2} = \frac{G_F^2 |V_{cq}|^2 p_P^3}{24\pi^3} |f_+(q^2)|^2, \quad (4)$$

where p_P is the three-momentum of pseudoscalar meson in the D rest frame, and $f_+(q^2)$ is a form-factor, whose normalization must be calculated theoretically, although its shape can be measured.

The BESIII experiment has taken about 2.9 fb^{-1} data at open-charm threshold during the 2010 and 2011 data runs. Using one-third of the data, a partially-blind analysis has been done with the $D^0 \rightarrow K e \nu$ and $D^0 \rightarrow \pi e \nu$ decays. Using the double tag technique, several hadronic D decays are fully reconstructed at first. The following four hadronic D decays are used: $D^0 \rightarrow K^- \pi^+$, $K^- \pi^+ \pi^0$, $K^- \pi^+ \pi^0 \pi^0$ and $K^- \pi^+ \pi^- \pi^+$. Mass peaks for the four hadronic tag modes are shown in Fig. 3. After hadronic D^0 tags are found, we reconstruct signal

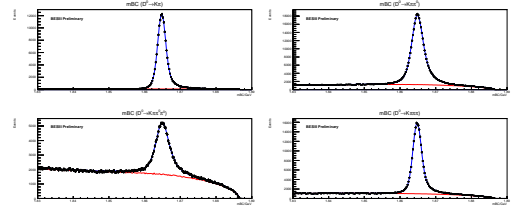


Figure 3: Distributions of the beam energy constraint masses for D^0 hadronic tags used for the $D^0 \rightarrow K e \nu$ and $\pi e \nu$ analyses. Modes in panels are $D^0 \rightarrow K^- \pi^+$, $K^- \pi^+ \pi^0$, $K^- \pi^+ \pi^0 \pi^0$ and $K^- \pi^+ \pi^- \pi^+$.

decay for the other \bar{D}^0 . The signal events with a missing ν are inferred using the variable $U = E_{miss} - |P_{miss}|$, similar to missing mass square, where "miss" here refers to the missing energy or momentum. Figure. 4 shows the U distributions and fit projections for the decays of $\bar{D}^0 \rightarrow K^+ e^- \nu$ and $\bar{D}^0 \rightarrow \pi^+ e^- \nu$.

Given the signal yields obtained from fitting U distributions and signal efficiencies obtained from signal Monte Carlo, the absolute branching fractions are obtained. Preliminary results of branching fractions are listed in Table 3, and comparisons with results from PDG2012 [9] and CLEO-c results [13] are also made. In order to measure form factor, partial decay rates are measured in different q^2 bins. $\bar{D}^0 \rightarrow K^+ e^- \nu$ candidates are divided into nine q^2 bins, while $\bar{D}^0 \rightarrow \pi^+ e^- \nu$ candidates are divided into seven q^2 bins. Signal yields in each q^2 bin are obtained by fitting U distributions in that q^2 range. Using an efficiency matrix versus q^2 , obtained from Monte-Carlo simulation, and combining with tag yields and tag efficiencies, the partial decay rates are obtained, as shown in Fig. 5. The values of q^2 -dependent form factors in each q^2 bin can be extracted from the measured partial decay rates as shown in Fig. 6. These data can be fitted with different parameterizations of the form factors, and the fit can distinguish between form

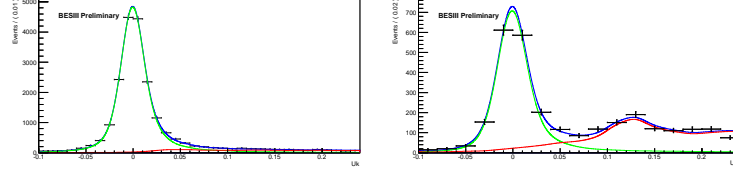


Figure 4: U distributions of $\bar{D}^0 \rightarrow K^+ e^- \nu$ (left) and $\bar{D}^0 \rightarrow \pi^+ e^- \nu$ (right). Blue, green, and red curves are the total fit, signal fit, and background fit, respectively.

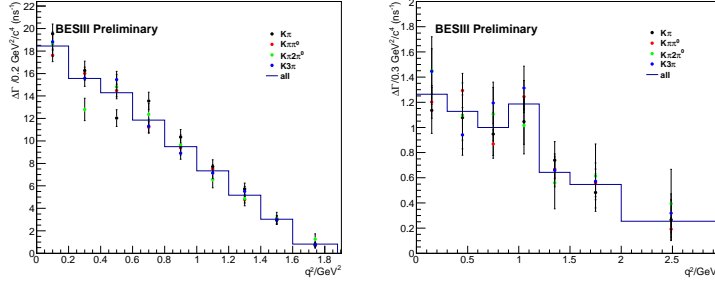


Figure 5: Partial decay rates measurement using individual tag modes (points) and all tag modes combined (histogram) for decay of $\bar{D}^0 \rightarrow K^+ e^- \nu$ (left) and $\bar{D}^0 \rightarrow \pi^+ e^- \nu$ (right).

Table 3: Branching fraction measurement using 923 pb⁻¹ of $\psi(3770)$ data from BESIII experiment, and comparisons with results from CLEO-c [13] and PDG2012 [9].

Experiment	$\mathcal{B}(\bar{D}^0 \rightarrow K^+ e^- \nu)(\%)$	$\mathcal{B}(\bar{D}^0 \rightarrow \pi^+ e^- \nu)(\%)$
BESIII	$3.542 \pm 0.030 \pm 0.067$	$0.288 \pm 0.008 \pm 0.005$
CLEO-c [13]	$3.50 \pm 0.03 \pm 0.04$	$0.288 \pm 0.008 \pm 0.003$
PDG2012 [9]	3.55 ± 0.04	0.289 ± 0.008

factors parameterizations. In general, one may express the form factors in terms of a dispersion relation, an approach that has been well established in the literature (see, for example, Ref. [14] and references therein):

$$f_+(q^2) = \frac{f_+(0)}{1 - \alpha (1 - q^2/m_{pole}^2)} + \frac{1}{\pi} \int_{(m_D+m_P)^2}^{\infty} \frac{Im(f_+(t))}{t - q^2 - i\epsilon} dt, \quad (5)$$

where m_{pole} is the mass of the lowest lying $(q_i \bar{q}_f)$ meson with the appropriate quantum numbers: for $D \rightarrow K e \nu$ it is D_s^{*+} and for $D \rightarrow \pi e \nu$ it is D^{*+} , the parameter α gives the relative contribution from the vector pole at $q^2 = 0$, m_D is the mass of the D meson, and m_P is the mass of the final state pseudoscalar meson. The integral term can be expressed in terms of an infinite series [14]. Typically it takes only a few terms to de-

scribe the data. Three different parameterizations of the form factor $f_+(q^2)$ are considered. The first parameterization, known as the simple pole model, is dominated by a single pole [15]; the second parameterization is known as the modified pole model [15]; the third parameterization is known as the series expansion [14]. Thus minimized χ^2 fits are employed to extract the values of $f_+(0)|V_{cd(s)}|$ using each of the parameterizations. The preliminary results for $f_+(0)|V_{cd(s)}|$ are shown in Table 4. With $|V_{cd}| = 0.2252$ ($|V_{cs}| = 0.97345$) [9] and BESIII new results (3 par. series) [16], we extract the values for $f_+^{D \rightarrow \pi}(0)$ and $f_+^{D \rightarrow K}(0)$, and results are compared with other experiments and theoretical calculations as shown in Fig. 7 [17].

4. Rare charm decays at BESIII: preliminary results on $D^0 \rightarrow \gamma \gamma$

Searches for rare-decay processes have played an important role in the development of the SM. Short-distance flavor-changing neutral current (FCNC) processes in charm decays are much more highly suppressed by the GIM mechanism than the corresponding down-type quark decays because of the large top quark mass. Observation of FCNC decays $D \rightarrow h l^+ l^-$ and $D \rightarrow l^+ l^-$ could therefore provide indication of new

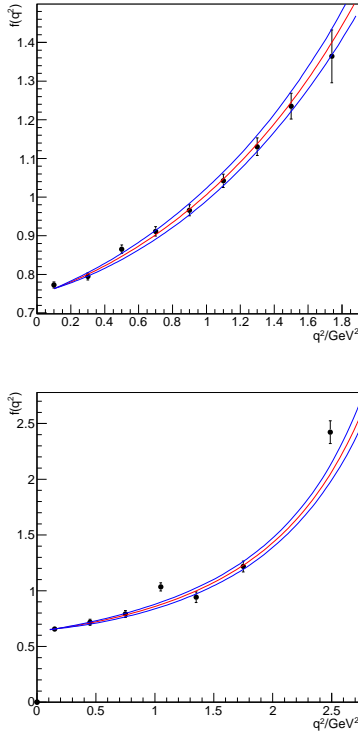


Figure 6: Plot of $f_+(q^2)$ from data with Lattice QCD prediction. Black points are from data with statistical error only, red curve is theoretical prediction, and blue curves are theoretical variations within statistical error only. The top plot is for $\bar{D}^0 \rightarrow K^+ e^- \nu$ and the bottom plot is for $\bar{D}^0 \rightarrow \pi^+ e^- \nu$ (bottom).

Table 4: Results of $f_+(0)|V_{cd(s)}|$ from individual form factor fits; statistical and systematic uncertainties on the least significant digits are shown in parentheses. Results from CLEO-c [13] are compared.

	$f_+(0) V_{cd(s)} $	
	BESIII	CLEO-c
3 par. Series		
$\bar{D}^0 \rightarrow K^+ e^- \nu$	0.729(8)(7)	0.726(8)(4)
$\bar{D}^0 \rightarrow \pi^+ e^- \nu$	0.144(5)(2)	0.152(5)(1)
2 par. Series		
$\bar{D}^0 \rightarrow K^+ e^- \nu$	0.726(6)(7)	0.717(6)(4)
$\bar{D}^0 \rightarrow \pi^+ e^- \nu$	0.140(4)(2)	0.145(4)(1)
Modified pole		
$\bar{D}^0 \rightarrow K^+ e^- \nu$	0.725(6)(7)	0.716(6)(4)
$\bar{D}^0 \rightarrow \pi^+ e^- \nu$	0.140(3)(2)	0.145(4)(1)
Simple pole		
$\bar{D}^0 \rightarrow K^+ e^- \nu$	0.729(5)(7)	0.720(5)(4)
$\bar{D}^0 \rightarrow \pi^+ e^- \nu$	0.142(3)(1)	0.146(3)(1)

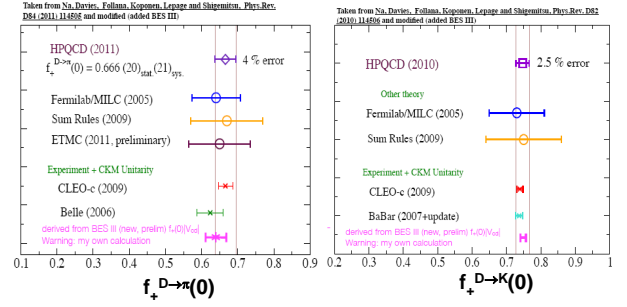


Figure 7: Comparison of $f_+(0)$ from experiments and theory. Left plot is for $f_+^{D \rightarrow \pi}(0)$, and right plot is for $f_+^{D \rightarrow K}(0)$. Note that BESIII result from D^0 decays only, while CLEO-c use both D^0 and D^+ decays [17].

physics or of unexpectedly large rates for long-distance SM processes like $D \rightarrow hV$, $V \rightarrow l^+ l^-$, with real or virtual vector meson V .

With 2.9 fb^{-1} data at $\psi(3770)$ peak, BESIII search for $D^0 \rightarrow \gamma\gamma$ decay which must be produced by FCNC. From the short distance contributions, the decay rate for $D^0 \rightarrow \gamma\gamma$ is predicted to be 3×10^{-11} [18, 19, 20]. However, the long distance contributions significantly enhance the decay rate which is estimated to be $(1 - 3) \times 10^{-8}$ [19, 20]. This decay could be enhanced by new physics (NP) effects which lead to contributions at loop level [21, 22]. For instance, in the framework of the Minimal Supersymmetric Standard Model (MSSM), the calculation shows that the decay rate for $c \rightarrow u\gamma$ transition could be 6×10^{-6} , which is one to two orders of magnitudes enhanced relative to the SM rate, by considering gluino exchange [21].

Experimental searches for $D^0 \rightarrow \gamma\gamma$ were performed by the CLEO [23] and BABAR [24] experiments based on data samples collected at the $\Upsilon(4S)$ peak. They found no significant signals. The latter experiment yields the most stringent experimental upper limit to date on the $\mathcal{B}(D^0 \rightarrow \gamma\gamma)$, 2.2×10^{-6} at 90% confidence level (C.L.).

Since one of the major backgrounds in the analysis of $D^0 \rightarrow \gamma\gamma$ comes from $D^0 \rightarrow \pi^0 \pi^0$, we firstly measure the decay rate of $D^0 \rightarrow \pi^0 \pi^0$ using the same data sample. Then we use the measured $D^0 \rightarrow \pi^0 \pi^0$ decay rate to do the normalization and background estimation for $D^0 \rightarrow \gamma\gamma$ measurement. Figure 8 shows the beam-constraint mass distribution of the observed $\pi^0 \pi^0$ signal events and comparison with MC simulations of the expected backgrounds. The fit to the beam-constraint mass yields 4081 ± 117 signal events. With the total reconstruction efficiency of 23.3%, the preliminary efficiency-corrected yield of $D^0 \rightarrow \pi^0 \pi^0$ based on our

$\psi(3770)$ data set is $17521 \pm 500(\text{stat}) \pm 1559(\text{syst})$ events (the estimation of the systematic uncertainty can be found in Ref. [25]).

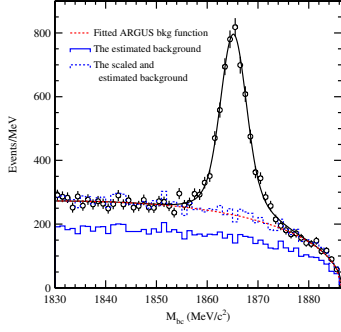


Figure 8: A fit to the $D^0 \rightarrow \pi^0 \pi^0$ candidate M_{bc} distribution based on the $\psi(3770)$ data sample. The black points are data, the black-smooth curve represents the overall fit (signal plus background), and the red-dashed curve corresponds to the fitted background shape. The blue-solid histogram represents the expected background shape and size based on our MC samples while the blue-dotted histogram is a fit to the data based on this expected MC-based background shape.

We analyze $D^0 \rightarrow \gamma\gamma$, and Fig. 9 shows ΔE distribution based on the $\psi(3770)$ data set, where ΔE is the energy difference between reconstructed energy of D meson and beam energy. The signal candidates should be peak near zero, therefore, no significant signal events are observed. We perform a maximum-likelihood fit to the ΔE distribution. In the fit, the signal shape is fixed by the corresponding MC shape. The background shape consists of three parts; MC-based shape to represent the contamination from $D^0 \rightarrow \pi^0 \pi^0$ whose size is also fixed based on our own observation; a 1st order polynomial that covers the contamination from Bhabha events which appear smoothly over the entire ΔE spectrum; a 1st order exponential polynomial, corresponding to the rest of the backgrounds. The fit yields -2.9 ± 7.1 signal events. This translates into an upper limit of 11 events at 90% C.L. based on the Bayesian method. Including the estimated total systematic uncertainty, we arrive at $\mathcal{B}(D^0 \rightarrow \gamma\gamma)/\mathcal{B}(D^0 \rightarrow \pi^0 \pi^0) < 5.8 \times 10^{-3}$ at 90% C.L.. With the known value of $\mathcal{B}(D^0 \rightarrow \pi^0 \pi^0)$ [9], this corresponds to $\mathcal{B}(D^0 \rightarrow \gamma\gamma) < 4.7 \times 10^{-6}$.

5. Conclusion

Since the start of running in 2008, BESIII has taken about 2.9 fb^{-1} of data at $\psi(3770)$. With peak luminosity

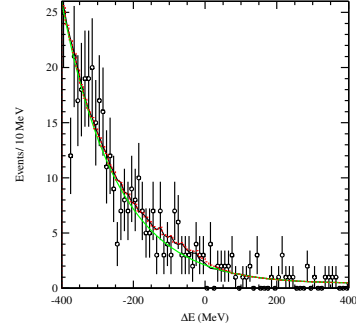


Figure 9: A fit to the $D^0 \rightarrow \gamma\gamma$ candidate ΔE distribution based on the $\psi(3770)$ data sample. Black points are data, solid black curve is the overall fitted curve (signal plus backgrounds), the red-dashed curve is the fitted total background, and the green curve is the exponential and linear polynomials.

reaching more than $6 \times 10^{32} \text{ cm}^{-2} \text{ s}^{-1}$ (60% of the designed luminosity), BESIII is poised to take more data at $\psi(3770)$ and in the higher (D_s) energy region. BESIII collaboration presented the most precise measurement for $D^+ \rightarrow \mu^+ \nu$ decay. Using part of the data, BESIII has presented preliminary results of the $D^0 \rightarrow K/\pi e \nu$ decays. Results from the full dataset and other modes are coming in the near future.

For the rare charm decay program, BESIII reported the search for $D^0 \rightarrow \gamma\gamma$ decay with single tag technique, and backgrounds are expected to be lower than experiment at B factories. While we are waiting for BESIII to take more data at $\sqrt{s} = 3.773 \text{ GeV}$, there is an alternate analysis approach that is unique to our data sample. The produced $\psi(3770)$ in our sample decays into a pair of $D^0 \bar{D}^0$. Reconstructing one of the D^0 mesons with known exclusive modes while searching for $D^0 \rightarrow \gamma\gamma$ in the other D^0 decay would yield an almost background-free environment, except for the irreducible contamination from $D^0 \rightarrow \pi^0 \pi^0$ for which we have control. Such a study is also currently under way. We also explore other rare charm decays in the future with more dataset at the BESIII experiment.

Acknowledgment

The author would like to thank his BESIII colleagues, Hajime Muramatsu, Chunlei Liu and Gang Rong for providing many plots and results in the paper. This work is supported in part by the National Natural Science Foundation of China under contract No. 11125525.

References

- [1] H. B. Li, Nucl. Phys. B (Proc. Suppl.) **162**, 312 (2006).
- [2] M. Kobayashi and T. Maskawa, Prog. Theor. Phys. **49**, 652 (1973).
- [3] L. Gibbons, hep-ex/0107079.
- [4] R. M. Baltrusaitis *et al.* (MARK-III Collaboration), Phys. Rev. Lett. **56**, 2140 (1986); J. Adler *et al.* (MARK-III Collaboration), Phys. Rev. Lett. **60**, 89 (1988).
- [5] M. Gronau, Y. Grossman, and J. L. Rosner, Phys. Lett. **B 508** (2001) 37.
- [6] D. M. Asner and W. M. Sun, Phys. Rev. **D73** (2006) 034024.
- [7] M. Ablikim *et al.* (BESIII Collaboration), Nucl. Instrum. Meth. A **614**, 345 (2010).
- [8] G. Rong (For BESIII Collaboration), *Pure leptonic charm decays*, talk given at CHARM2012.
- [9] J. Beringer *et al.* (Particle Data Group), Phys. Rev. D **86**, 010001 (2012).
- [10] B. I. Eisenstein *et al.* (CLEO Collaboration), Phys. Rev. D **78**, 052003 (2008).
- [11] E. Follana *et al.* (HPQCD and UKQCD Collaborations), Phys. Rev. Lett. **100**, 062002 (2008).
- [12] M. Artuso, *Status and future perspectives on V_{cs} and V_{cd}* , *Experimental*, presented at 4th Int. Workshop on the CKM Unitarity Triangle, Dec., 2006, Nagoya, Japan.
- [13] D. Besson *et al.* (CLEO Collaboration), Phys. Rev. D **80**, 032005 (2009).
- [14] T. Becher and R. J. Hill, Phys. Lett. B **633**, 61 (2006).
- [15] D. Becirevic and A. B. Kaidalov, Phys. Lett. B **478**, 417 (2000).
- [16] C. L. Liu (For BESIII Collaboration), *Review of semileptonic charm decays*, talk given at CHARM2012.
- [17] J. Rademacker, *“Semileptonic Charm Decays”*, talk given at FPCP2012.
- [18] C. Greub, T. Hurth, M. Misiak, and D. Wyler, Phys. Lett. B **382**, 415 (1996).
- [19] S. Fajfer, P. Singer, and J. Zupan, Phys. Rev. D **64**, 074008 (2001).
- [20] G. Burdman, E. Golowich, J. L. Hewett, and S. Pakvasa, Phys. Rev. D **66**, 014009 (2002).
- [21] S. Prelovsek and D. Wyler, Phys. Lett. B **500**, 304 (2001).
- [22] A. Paul, I. I. Bigi, and S. Recksiegel, Phys. Rev. D **82**, 094006 (2010).
- [23] T. E. Coan *et al.* (CLEO Collaboration), Phys. Rev. Lett. **90**, 101801 (2003).
- [24] J. P. Lees *et al.* (BABAR Collaboration), Phys. Rev. D **85**, 091107 (R) (2012).
- [25] H. Muramatsu (for BESIII Collaboration), *Search for $D^0 \rightarrow \gamma\gamma$ decays*, talk given at CHARM2012.